

# Mutant p53 in Concert With an Interleukin-27 Receptor Alpha Deficiency Causes Spontaneous Liver Inflammation, Fibrosis, and Steatosis in Mice

Denada Dibra,<sup>1</sup> Xueqing Xia,<sup>1</sup> Abhisek Mitra,<sup>1</sup> Jeffrey J. Cutrera,<sup>1</sup> Guillermina Lozano,<sup>2</sup> and Shulin Li<sup>1</sup>

The cellular and molecular etiology of unresolved chronic liver inflammation remains obscure. Whereas mutant p53 has gain-of-function properties in tumors, the role of this protein in liver inflammation is unknown. Herein, mutant p53<sup>R172H</sup> is mechanistically linked to spontaneous and sustained liver inflammation and steatosis when combined with the absence of interleukin-27 (IL27) signaling (IL27RA), resembling the phenotype observed in nonalcoholic fatty liver disease (NAFLD) and nonalcoholic steatohepatitis (NASH) patients. Indeed, these mice develop, with age, hepatocyte necrosis, immune cell infiltration, fibrosis, and micro- and macrosteatosis; however, these phenotypes are absent in mutant p53<sup>R172H</sup> or IL27RA<sup>-/-</sup> mice. Mechanistically, endothelin A receptor (ETAR)-positive macrophages are highly accumulated in the inflamed liver, and chemical inhibition of ETAR signaling reverses the observed phenotype and negatively regulates mutant p53 levels in macrophages. **Conclusion:** The combination of mutant p53 and IL27RA<sup>-/-</sup> causes spontaneous liver inflammation, steatosis, and fibrosis *in vivo*, whereas either gene alone *in vivo* has no effects on the liver. (HEPATOLOGY 2016;63:1000-1012)

The most commonly mutated gene in cancer cells is the oncogene, p53. Many investigators have shown *in vivo* that mice carrying mutant p53 in a Li-Fraumeni mouse model spontaneously develop a tumor profile with metastatic disease that is different from mice carrying null p53.<sup>(1,2)</sup> Aside from the most commonly known function of oncogenes in propelling tumor progression, a new notion of *oncogene-induced inflammation* or *oncogene-sustained inflammation* in modulating human disease is emerging.<sup>(3)</sup>

Indeed, one of the mutant p53 gain-of-function properties was attributed to chronic nuclear factor kappa B activation upon the inflammatory stimuli of tumor necrosis factor (TNF) in cultured cancer cells and *in vivo*.<sup>(4-8)</sup> Though these mutant p53 mice do not develop spontaneous inflammatory disease, they are highly susceptible to dextran sulfate sodium-associated colitis and inflammation-associated colorectal cancer.<sup>4</sup>

Chronic liver inflammation can result in the deadly diseases, such as cirrhosis and hepatocellular carcinoma

*Abbreviations:* BSA, bovine serum albumin; cDNA, complementary DNA; Ct, cycle threshold; CTGF, connective tissue growth factor; Cy7, cyanine 7; ELISA, enzyme-linked immunosorbent assay; ETAR, endothelin A receptor; FCM, flow cytometry; GAPDH, glyceraldehyde 3-phosphate dehydrogenase; HCC, hepatocellular carcinoma; H&E, hematoxylin and eosin; IF, immunofluorescence; IHC, immunohistochemistry; IL27, interleukin-27; IL27RA, IL27 receptor  $\alpha$ ; KCs, Kupffer cells; LPS, lipopolysaccharide; MDM2, murine double minute 2; NAFLD, nonalcoholic fatty liver disease; NASH, nonalcoholic steatohepatitis; NK, natural killer; NKT, natural killer T cells; PE, phycoerythrin; pERK1/2, phosphorylated extracellular signal-regulated protein kinases 1 and 2; rIL27, recombinant IL27; RT-PCR, reverse transcriptase polymerase chain reaction; SH, steatohepatitis; TNF, tumor necrosis factor; WT, wild type.

Received June 1, 2015; accepted November 17, 2015.

Additional Supporting Information may be found at [onlinelibrary.wiley.com/doi/10.1002/hep.28379/suppinfo](http://onlinelibrary.wiley.com/doi/10.1002/hep.28379/suppinfo).

This study was supported by NIH RO1 DK102767-01a1.

Copyright © 2015 by the American Association for the Study of Liver Diseases

View this article online at [wileyonlinelibrary.com](http://wileyonlinelibrary.com).

DOI 10.1002/hep.28379

Potential conflict of interest: Nothing to report.

(HCC). Spontaneous hepatocyte apoptosis, infiltration of inflammatory cells, and compensatory proliferation are the initial steps in sustaining chronic liver inflammation, which, when left unresolved, results in fibrosis. Although knowledge of the key players that spontaneously drive this process is limited, the evidence suggests that whichever role p53 plays, it is an important one. Many investigators have shown that p53 protein accumulates in patients with various inflammatory liver diseases.<sup>(9-12)</sup> Mechanistically, Kodama et al. increased p53 expression in hepatocytes by deleting murine double minute 2 (MDM2; the enzyme that binds and degrades p53), which promoted fibrosis by inducing connective tissue growth factor (CTGF) expression.<sup>(13)</sup> Meanwhile, another group has shown that p53 expression in activated stellate cells will limit liver fibrosis by inducing cell death of these cells.<sup>(14)</sup> Because the role of mutant p53 in inflammation is so poorly understood, one imminent question is whether endogenous mutant p53 has any effect in liver inflammation and fibrosis. If so, under what circumstance mutant can p53 affect liver problems such as spontaneous inflammation, fibrosis, and/or fatty liver given that mice carrying mutant p53 gene do not develop any liver abnormalities?<sup>(2)</sup>

The role of interleukin-27 (IL27) in modulating the shape and strength of the immune response has been well appreciated. This cytokine possesses either pro- or anti-inflammatory functions in a context-dependent manner.<sup>(15)</sup> IL27 is tightly involved in liver disease; mice absent in IL27 receptor  $\alpha$  (IL27RA) signaling are highly sensitive to liver inflammation, concavalin A-induced liver disease, or lipopolysaccharide (LPS) stimulation, albeit these mice are inflammation free in absence of stimuli.<sup>(16,17)</sup> We hypothesized that p53<sup>515A</sup> “knock-in” mice carrying one germline mutant p53 allele encoding p53R172H (heterozygote, referred as p53<sup>H/+</sup> from herein), the mouse equivalent of the human hotspot mutant p53R175H, plus mice IL27RA knockout signaling might spontaneously develop liver

disease. Indeed, these mice (IL27RA<sup>-/-</sup>p53<sup>H/+</sup>) mice spontaneously develop hepatocyte necrosis, immune cell infiltration fibrosis, and fatty liver with age, whereas neither IL27RA<sup>-/-</sup> nor p53<sup>H/+</sup> mice develop any of these phenotypes. Of interest is one particular population of immune cell, endothelin A receptor (ETAR)-positive macrophages, which increasingly accumulate in the inflamed liver. Chemical inhibition of ETAR signaling reverses the inflammatory phenotype observed in these mice, suggesting that mutant p53 and absence of IL27 signaling results in liver inflammation and steatosis by ETAR-positive macrophages.

## Materials and Methods

### TRANSGENIC MICE

All mice strains were maintained in a C57Bl/6 cohort. IL27RA<sup>-/-</sup> mice and P53<sup>H/+</sup> mice were bred to create cohorts. IL27RA<sup>-/-</sup> mice were previously donated by Dr. Frederic de Sauvage (Genentech Inc., South San Francisco, CA). Genotyping was performed as described below for both p53 and IL27RA. For the cohort studies, mice were euthanized once they reached euthanasia criteria mainly because of tumor burden. For the time-course study, mice from each genotype were euthanized at the indicated times. Liver tissue was fixed in neutralized paraformaldehyde before sectioning. To inhibit ETAR signaling, Zibotentan (ZD4054; Selleck Chemicals, Houston, TX), 5 mg/kg/mouse, or vehicle control was given intraperitoneally to mice three times a week starting at age 3 months, diluted at 100  $\mu$ L of saline per mouse. The drug was given to mice for 8 consecutive weeks. Consequently, mice were euthanized by CO<sub>2</sub> asphyxiation, and liver tissue was used for further studies. All the procedures involving animals were approved by the institutional animal care and use committee.

#### ARTICLE INFORMATION:

From the Department of <sup>1</sup>Pediatrics and <sup>2</sup>Department of Genetics, The University of Texas MD Anderson Cancer Center, Houston, TX

#### ADDRESS CORRESPONDENCE AND REPRINT REQUESTS TO:

Shulin Li, Ph.D.  
The University of Texas Graduate School of  
Biomedical Sciences at Houston  
The University of Texas MD Anderson Cancer Center

1515 Holcombe Boulevard  
Houston, TX 77030.  
E-mail: sli4@mdanderson.org  
Fax: 713-763-9607.

## WESTERN BLOTTING

Briefly, liver tissue was snap frozen in liquid nitrogen. Tissue was homogenized in lysis buffer, and supernatants were quantified for protein amount.<sup>(18)</sup> Next, 160  $\mu$ g of cell lysate was loaded in 10% sodium dodecyl sulfate/polyacrylamide gel electrophoresis, transferred to a nitrocellulose membrane, and incubated with primary antibody overnight at 4°C (1,000 $\times$  dilution for anti-p53; Novus, Littleton, CO), 2,500 $\times$  anti-GAPDH (glyceraldehyde 3-phosphate dehydrogenase), 5,000 $\times$  anti-mouse immunoglobulin G/horseradish peroxidase (Santa Cruz Biotechnology, Santa Cruz, CA), 500 $\times$  anti-pERK1/2 (phosphorylated extracellular signal-regulated protein kinases 1 and 2; Santa Cruz Biotechnology), and 500 $\times$  anti-MDM2 (Santa Cruz Biotechnology).

## PICRIUS RED STAINING

Picosirius red staining was performed according the manufacturer's instructions (IHC World, Woodstock, MD).

## HEMATOXYLIN AND EOSIN STAINING OF LIVER SECTIONS AND SCORING OF LIVER LESIONS

Sections of paraffin-embedded tissues were stained with hematoxylin and eosin (H&E). Pathological readings were scored by a pathologist at our institution. Images were taken with a Nikon Eclipse Ti microscope (Nikon, Tokyo, Japan). During time-course experiments, lesions were counted under a 200 $\times$  microscope, where 15 fields per slide were counted. Small lesions typically observed early in the liver consisted of hepatocellular degeneration and hepatocyte necrosis along with Kupffer cell (KC) hyperplasia attended by a small number of lymphocytes were quantified as previously described.<sup>(19)</sup>

## GENOTYPING

DNA was extracted from ear tissue, and polymerase chain reaction (PCR) for p53 gene was performed using the primer sequence as previously described by Lang et al.<sup>(2)</sup> The presence of IL27RA gene was confirmed by using forward CAAGAAGAGGTCCCGTGCTG primer sequence and reverse TTGAGCCCAGTCCA CCACAT sequence. PCR primers for the absence of

IL27RA are as follows: GCTTTCGTCTCCCGTG TGCT (forward) and TGAGCCCAGAAAGCGAA GGA (reverse).

## QUANTITATIVE REAL-TIME PCR

Samples were prepared and processed as previously described.<sup>(20)</sup> Briefly, total RNA was isolated from cells using TRIzol Reagent (Life Technologies, Carlsbad, CA). Residual genomic DNA was removed from total RNA using the TURBO DNA-free kit (Life Technologies). Two micrograms of RNA were used for complementary DNA (cDNA) synthesis using the High-Capacity RNA-to-cDNA Kit (Life Technologies). Relative gene expression levels were determined using reverse-transcriptase quantitative PCR (RT-PCR) and the SYBR Green labeling method in a StepOnePlus Real-Time PCR System (Life Technologies). The reaction contained 2  $\mu$ L of cDNA, 12.5  $\mu$ L of SYBR Green PCR Master Mix (Life Technologies), and 200  $\mu$ M of primer in a total volume of 25  $\mu$ L. PCR cycling conditions were as follows: 40 cycles of 15 seconds at 95°C and 60 seconds at 60°C. All samples were run in duplicates. The cycle threshold (Ct) value of each sample was acquired, and the relative level of gene expression was calculated by the delta Ct method, which was normalized to the endogenous control of GAPDH. Data are expressed as n-fold relative to control. The primer sequences for the mouse GAPDH and P53 are: Gapdh CCAGCCTCGTCC CGTAGAC and CGCCAATACGGCCAAA; P53 CTCTCCCCCGCAAAGAAAAA and CGG AACATCTCGAAGCGTTA.

## STATISTICAL ANALYSIS

The Student *t* test was used to analyze the differences among groups. GraphPad Prism for Windows was used to prepare and analyze graphs (GraphPad Software Inc., La Jolla, CA).

## FLOW CYTOMETRY ANALYSIS

Purified liver immune infiltrates were blocked for nonspecific staining in 2% bovine serum albumin (BSA) and with anti-CD16 (5  $\mu$ g/mL) for 20' at 4°C. Afterward, cells were stained in 2% BSA with CD4-Violet421 (1:100; Pharminogen, San Diego, CA), CD8/ phycoerythrin (PE)/cyanine 7 (Cy7) (1:100; BioLegend, San Diego, CA), F4/80-FITC (fluorescein isothiocyanate) (1:100; eBioscience, Inc., San Diego,

CA), CD3-e450 (eBioscience), NK1.1-PE-Cy7 (eBioscience), CD19-Violet421 (1:100; BioLegend) and B220-PerCP (1:100; BioLegend), CD11c-Violet 421 (1:100, BioLegend), and MHCII-PerCP (1:100; BioLegend). Last, cells were washed twice in 2% BSA and analyzed by flow cytometry (FCM) using Attune (Invitrogen, Carlsbad, CA) and FlowJo (Tree Star, Inc., Ashland, OR).

## ENZYME-LINKED IMMUNOSORBENT ASSAY

Enzyme-linked immunosorbent assay (ELISA) for TNF (eBioscience) and IL6 (BioLegend) was performed according to the manufacturer's instructions. Briefly, liver tissue was processed as described in a western blotting procedure and the supernatant was quantified for both total protein amount and levels of cytokines by ELISA. Cytokine levels were normalized per total protein amount.

## Results

To understand the impact of mutant p53 in liver disease, we choose a mouse model of patients with Li Fraumeni-like syndrome. These mice carry a germline mutant p53 allele encoding p53R172H, the mouse equivalent of the human hotspot mutant, p53R175H.<sup>(2)</sup> Because these mice do not develop spontaneous liver abnormalities, we crossed mutant p53 carrying either one knock-in allele of p53R172H (p53<sup>H/+</sup>) or two knock-in alleles of p53R172H (p53<sup>H/H</sup>) to IL27RA<sup>-/-</sup> mice given that these mice are more susceptible to inducible liver inflammation. Mice of different groups (C57Bl/6 [wild-type; WT], IL27RA<sup>-/-</sup>, p53<sup>H/H</sup>, p53<sup>H/+</sup>, IL27RA<sup>-/-</sup>p53<sup>H/+</sup>, and IL27RA<sup>-/-</sup>p53<sup>H/H</sup>) were monitored over time. Once IL27RA<sup>-/-</sup>p53<sup>H/H</sup> and IL27RA<sup>-/-</sup>p53<sup>H/+</sup> mice became moribund, livers of these mice and those from control age-matched groups were analyzed and compared. Livers in aged WT, IL27RA<sup>-/-</sup>, and p53<sup>H/+</sup> mice did not contain any abnormalities (Fig. 1A); however, IL27RA<sup>-/-</sup>p53<sup>H/+</sup> mice spontaneously developed liver abnormalities with an increased accumulation of inflammatory cells in livers (Fig. 1A). Grossly, mice developed a different phenotype, ranging from enlarged livers to mild or severe steatosis (Fig. 1B). Meanwhile, these mice also developed large necrotic areas, extensive fibrosis, hepatocellular degeneration, and both micro- and macrovesicular steatosis, bile accumulation, or hemorrhage (Fig. 1C). More than

75% of IL27RA<sup>-/-</sup>p53<sup>H/+</sup> mice developed these liver abnormalities, whereas all of the control mice had normal livers (Fig. 1D). Pathological readings for fibrosis and collagen deposition were further confirmed by Sirius Red staining (Fig. 1E). Mice with more advanced liver disease developed both fat accumulation and fibrosis in livers, consistent with patients with nonalcoholic steatohepatitis (NASH; Supporting Fig. 1). Whereas chronic inflammation was a suspected phenotype, steatosis was an unexpected observation, although studies have implicated KCs in liver steatosis.<sup>(22)</sup>

Different from IL27RA<sup>-/-</sup>p53<sup>H/+</sup> mice, IL27RA<sup>-/-</sup>p53<sup>H/H</sup> mice carrying both mutant p53 alleles developed liver inflammation at a lower frequency than IL27RA<sup>-/-</sup>p53<sup>H/+</sup> mice (less than 3% when compared to 75%). Such reduced frequency may be attributed to the shorter life span in these mice because of succumbing to tumor burden at an early age (between 4 and 7 months of age), whereas IL27RA<sup>-/-</sup>p53<sup>H/+</sup> mice survive for 14–18 (referred as “aged mice” throughout this work) months, allowing a longer time span for chronic liver inflammation to occur.

Next, livers of younger mice, ages 2 and 4 months, were analyzed to understand the early events that led to liver fibrosis and steatosis in our model. Indeed, a higher frequency of IL27RA<sup>-/-</sup>p53<sup>H/+</sup> mice developed inflammatory foci in the liver when compared to other groups (Fig. 2A,B). Liver damage and compensatory proliferation are prerequisites for inflammatory cell infiltration; thus, the increase in the number of Ki67-positive cells in livers of IL27RA<sup>-/-</sup>p53<sup>H/+</sup> mice was expected (Fig. 2C–D). These results indicate that compensatory proliferation and accumulation of immune cells are early events leading to the phenotype observed in these older mice.

Because accumulation of immune cells is an early event in IL27RA<sup>-/-</sup>p53<sup>H/+</sup> mice, we wished to investigate which immune cells are most likely involved in this process. Intrahepatic immune cells were profiled by FCM in mice at 3 months of age (because inflammatory foci were consistently observed in 2- and 4-month-old mice). Others have found that natural killer (NK) T (NKT) cells, KCs, CD4 T cells, and NK cells play an important role in liver inflammation.<sup>(23)</sup> In immune cell profiling among different groups at age 3 months, no significant changes were noted in immune cell subgroups among all genotypes (Fig. 3A). However, as the mice age, the number of F4/80-positive cells were significantly increased in livers of IL27RA<sup>-/-</sup>p53<sup>H/+</sup> mice when compared to controls (Fig. 3B,C).

F4/80 is a hallmark of KCs, which are involved in liver pathogenesis induced by multiple individual

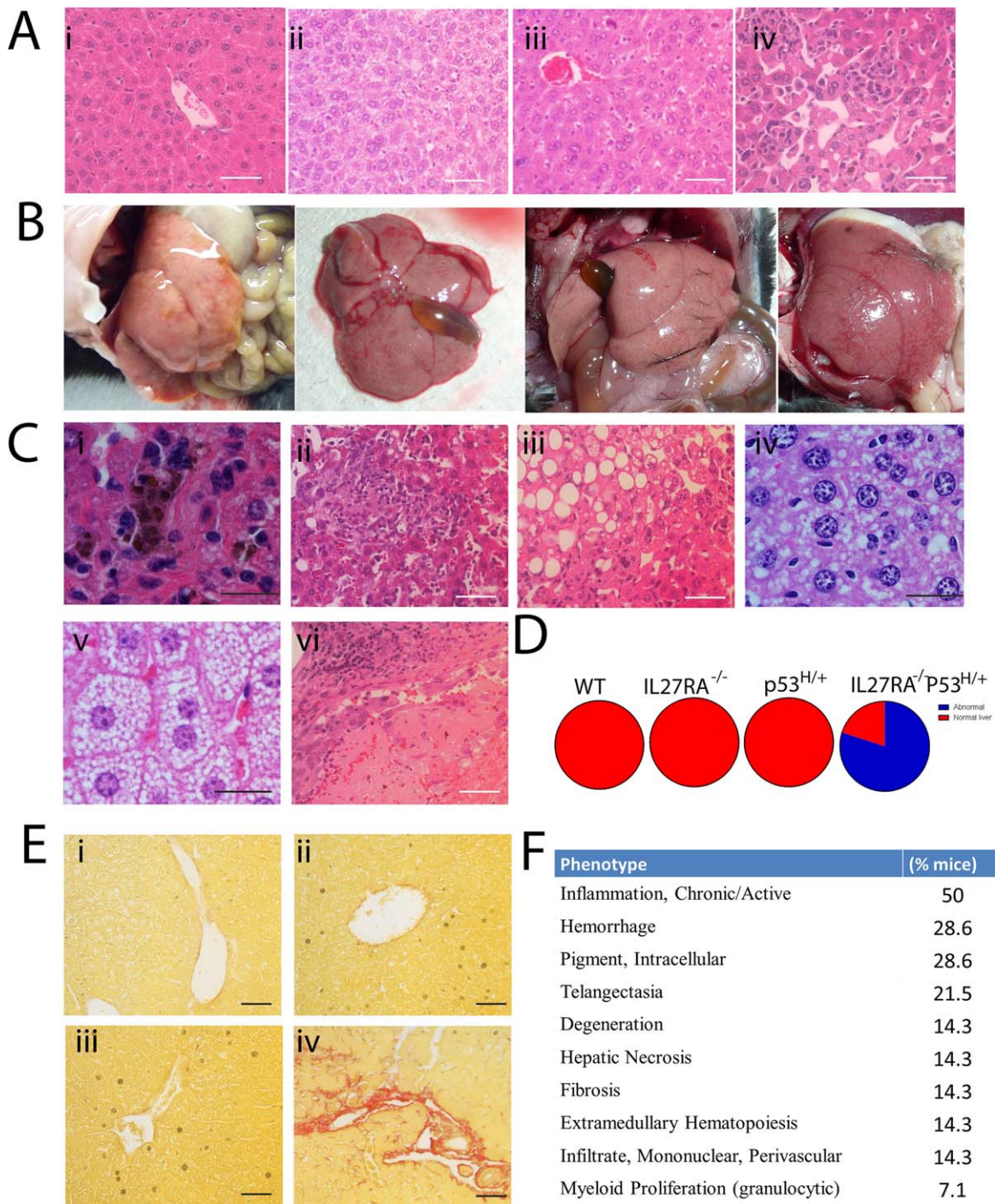


**FIG. 1.** Combination of mutant p53 and IL27RA<sup>-/-</sup> causes spontaneous liver inflammation and steatosis. (A) Representative H&E staining of livers of 12-16 months of age of (i) WT, (ii) IL27RA<sup>-/-</sup>, (iii) p53<sup>H/+</sup>, or (iv) IL27RA<sup>-/-</sup>p53<sup>H/+</sup>. White scale bar, 50  $\mu$ m. (B) Representative photomicrographs of gross livers of IL27RA<sup>-/-</sup>p53<sup>H/+</sup>. (C) Representative H&E staining for (i) pigment accumulation, (ii) necrotic area surrounded by immune infiltrates, (iii-v) macro- and microsteatosis, and (vi) hemorrhage. White scale bar, 50  $\mu$ m. Black scale bar, 25  $\mu$ m. (D) Quantification of the percentage of mice that developed liver-related inflammation: WT (N = 5); IL27RA<sup>-/-</sup> (N = 8); and p53<sup>H/+</sup> (N = 8); IL27RA<sup>-/-</sup>p53<sup>H/+</sup> (N = 18). Lymphomas were excluded as a phenotype. (E) Fibrosis was assessed based on Sirius red staining of (i) WT, (ii) IL27RA<sup>-/-</sup>, (iii) p53<sup>H/+</sup>, or (iv) IL27RA<sup>-/-</sup>p53<sup>H/+</sup> age-matched mice. (F) Percentage of mice IL27RA<sup>-/-</sup>p53<sup>H/+</sup> developing liver-related abnormalities based on pathological readings. N = 18.

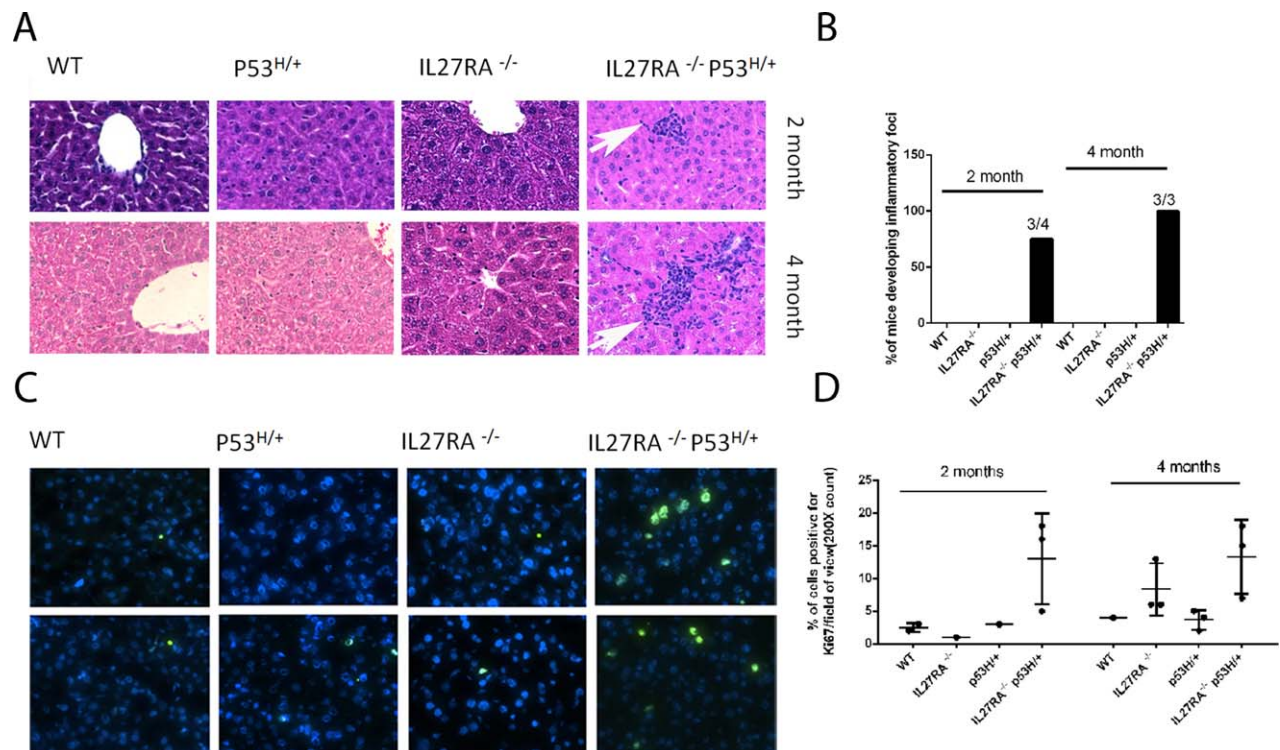


**FIG. 2.** Liver inflammation and compensatory proliferation are early events in liver pathogenesis. (A and B) Time-course study showing liver pathology and quantification in mice as early as 2 and 4 months in IL27RA<sup>-/-</sup>p53<sup>H/+</sup> evaluated by H&E staining. N = 3–4 per group. Pictures taken at 200 $\times$ . (C and D) Time-course study showing Ki67 staining and quantification in liver of 2- and 4-month-old mice of different genotypes. Dots indicate data from liver of individual mice. Pictures taken at 200 $\times$ .

stressors, such as chemicals, toxins, CCL<sub>4</sub>, and endotoxins, mainly through release of cytokines, superoxides, and nitric oxide. Because F4/80 cells were significantly increased in the inflammatory-prone IL27RA<sup>-/-</sup>p53<sup>H/+</sup> mice, we sought to define any signaling changes observed in these cells. Others have previously reported that endothelin/endothelin receptor axis to be involved in CCL<sub>4</sub>-mediated liver fibrosis.<sup>(24)</sup> Interestingly, ETAR was highly and significantly up-regulated in macrophages in the liver of the aged IL27RA<sup>-/-</sup>p53<sup>H/+</sup> when compared with other cohorts, suggesting the involvement of ETAR-positive KCs in sustaining an unresolved chronic inflammation (Fig. 4A). In supporting this notion, ET1, the ligand for this receptor, was also elevated in macrophages of these aged mice (Fig. 4B). Similar elevations are observed in cirrhosis patients when compared to healthy ones.<sup>(25)</sup>

One interesting question is whether IL27 can directly affect ETAR levels in myeloid cells. To test this hypothesis, myeloid cells were used because these cells contain

detectable levels of endogenous ETAR expression. In agreement with the *in vivo* observation, treatment with recombinant IL27 reduced the level of ETAR expression in these myeloid cells (Supporting Fig. 2). Furthermore, because ETAR levels are not detectable in KCs after treatment with LPS *in vivo*, the isolated primary KCs from these mice were restimulated with LPS *in vitro* in the presence or absence of recombinant IL27 (rIL27) overnight. Indeed, rIL27 inhibited LPS to induce ETAR levels (Supporting Fig. 3). And, last, to better understand whether IL27 can inhibit ETAR levels *in vivo* under inflammatory conditions, WT and IL27RA<sup>-/-</sup> mice were treated *in vivo* with CCL<sub>4</sub> and these fibrotic liver specimens were analyzed for ETAR levels (Supporting Fig. 4). As expected, ETAR levels were higher in liver of IL27RA<sup>-/-</sup> mice when compared to the WT ones, further suggesting the involvement of IL27 in regulation of ETAR.

To establish whether these ETAR macrophages indeed regulate establishment and sustaining of inflammation, ZD4054, a chemical inhibitor of

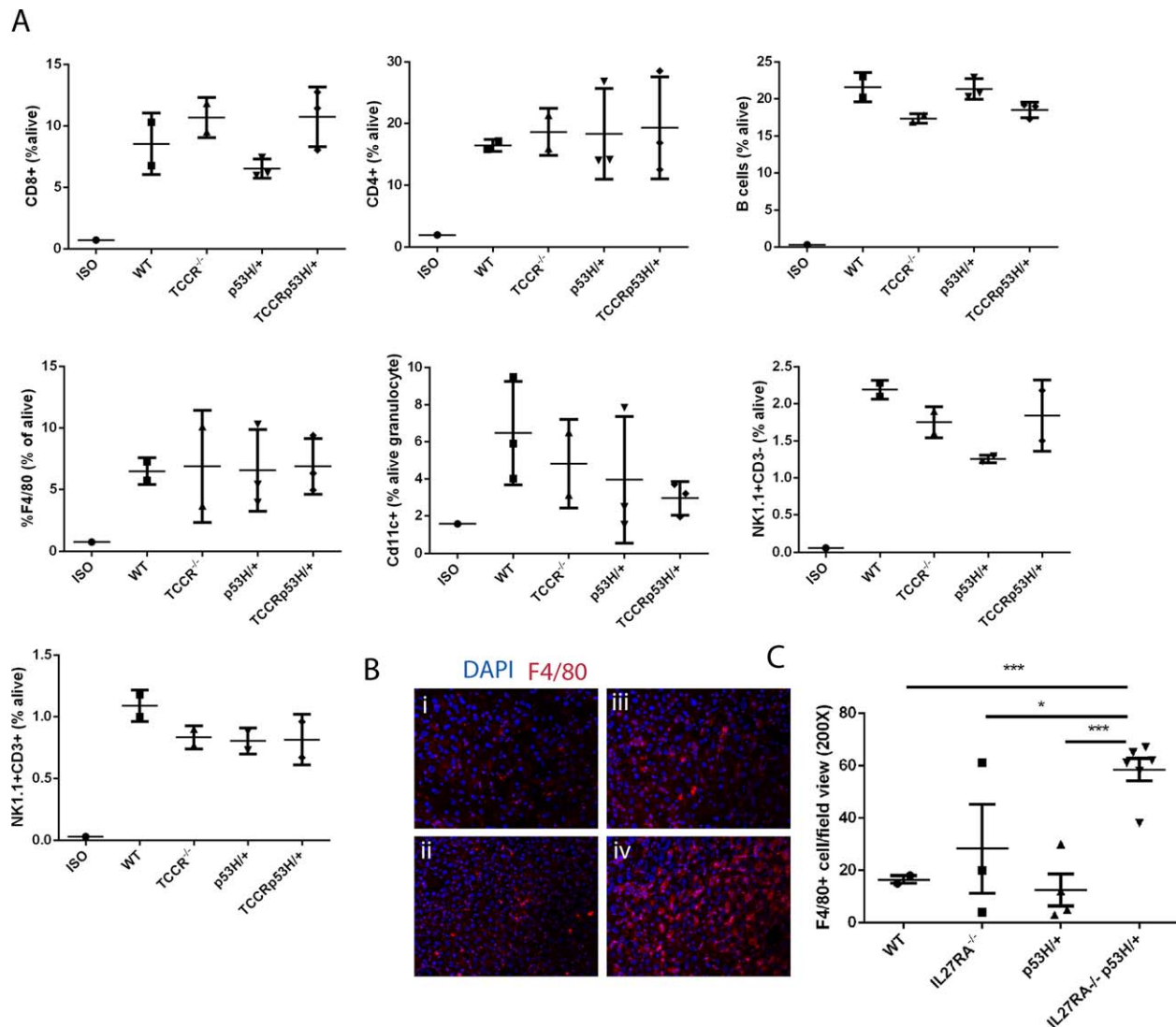


**FIG. 3.** Increased number of macrophages associated with liver disease phenotype. (A) No significant changes were observed in mice of different genotypes in CD4, CD8, B, NK, NKT, macrophages, or CD11c cells in liver of 3-month-old mice analyzed by FCM. (B and C) Significantly enhanced number of F4/80-positive in aged IL27RA<sup>-/-</sup> p53<sup>H/+</sup> mice when compared to an age-matched control one analyzed by IHC. Dots indicate data from the liver of individual mice. Pictures taken at 200X. \*P < 0.05. Abbreviation: DAPI, 4',6-diamidino-2-phenylindole.

ETAR signaling, was used. Once IL27RA<sup>-/-</sup> p53<sup>H/+</sup> mice reached 3 months of age, these mice were treated with ZD4054 or sham for 8 consecutive weeks. Because ET1/ETAR signaling induces pERK1/2 activation, we sought to determine whether ZD4054 inhibits ET1/ETAR-induced pERK1/2 in macrophages. Indeed, both immunohistochemistry (IHC) and western blotting results confirmed that ZD4054 inhibited ETAR-mediated downstream signaling (Fig. 4C,D). H&E staining of the livers of IL27RA<sup>-/-</sup> p53<sup>H/+</sup> mice treated with ZD4054 inhibitor showed a

significant reduction in the number of inflammatory foci and early signs of steatosis in the liver (Fig. 4E,F).

The above result led us to hypothesize that enhanced ETAR signaling sustains an inflammatory phenotype in macrophages of livers. IL6 and TNF are two of the most dominant inflammatory cytokines involved in patients with NASH liver pathogenesis.<sup>(5,26)</sup> Triple staining for ETAR, F4/80, and TNF showed that inhibition of ETAR signaling reduced significantly TNF levels in ETAR-positive macrophages (Fig. 5A,B) when compared to controls.

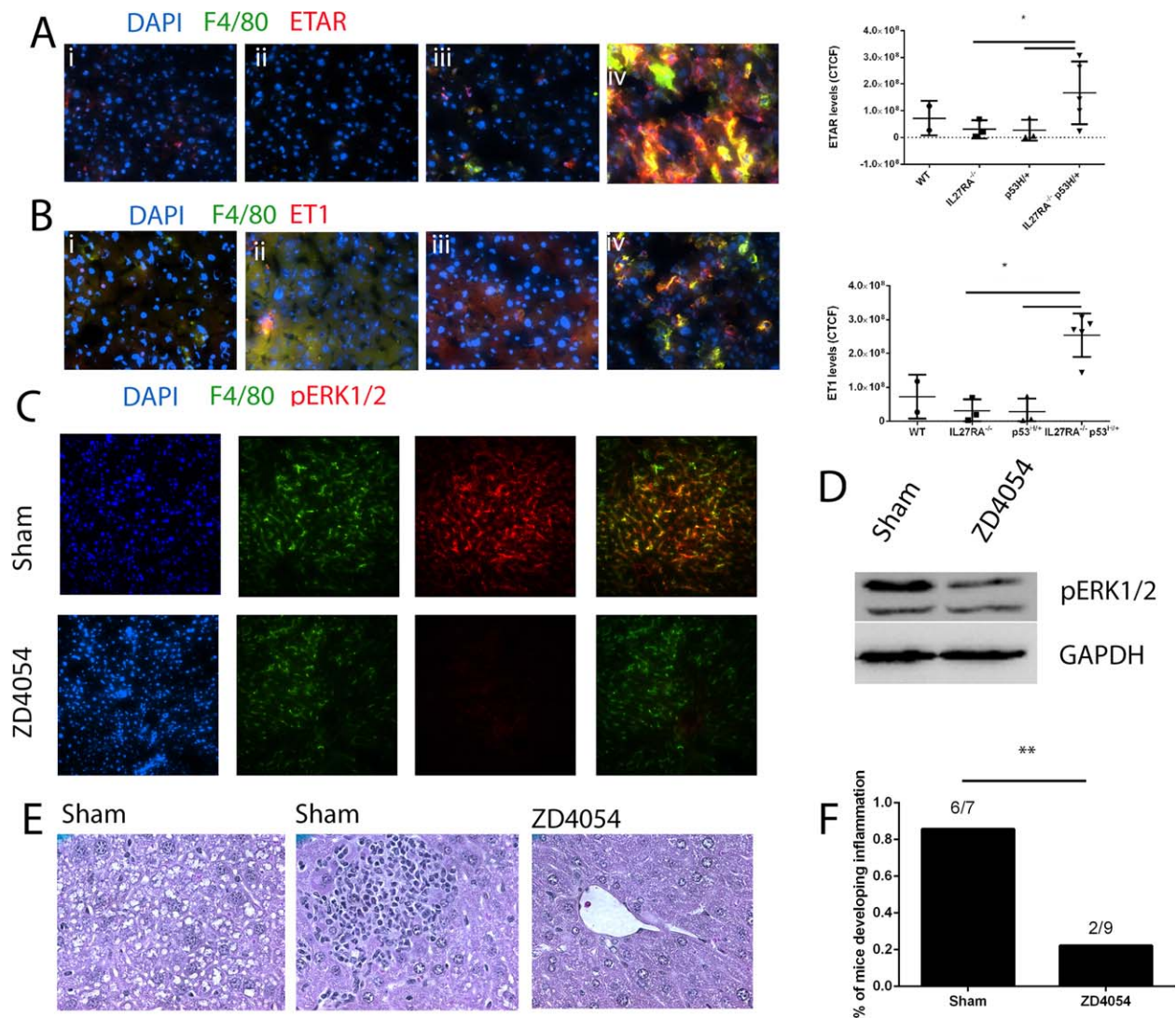


**FIG. 4.** ETAR-positive macrophages are responsible for inflammatory response in these mice. (A) Dual staining for ETAR and F4/80 and ETAR quantification in different genotypes showed that ETAR-positive macrophages are highly accumulated in liver of aged mice. (B) Dual staining for ET1 and F4/80 and ET1 quantification in different genotypes showed that ET1-positive macrophages are highly accumulated in liver of aged mice. (C and D) IF and western blotting analysis showing that the chemical inhibitor of ETAR signaling, ZD4054, repressed the downstream signaling of ETAR and pERK1/2 in macrophages. (E and F) Photomicrograph and quantifications showing reducing in inflammation in steatosis in IL27RA<sup>-/-</sup>p53<sup>H/+</sup> mice treated with ZD4054 (N = 9), when compared to sham treated mice (N = 7). Chi-square test was used to determine the differences among these two groups. *In vivo* data with ZD4054 inhibitor was repeated twice with similar results. (i) WT, (ii) IL27RA<sup>-/-</sup>, (iii) p53<sup>H/+</sup>, or (iv) IL27RA<sup>-/-</sup>p53<sup>H/+</sup>. Dots indicate data from liver of individual mice. Pictures taken at 200×. \**P* < 0.05. Abbreviation: DAPI, 4',6-diamidino-2-phenylindole.

Similarly, triple staining for ETAR, F4/80, and IL6 showed that inhibition of ETAR signaling significantly reduced IL6 levels in ETAR-positive macrophages in the inflammatory prone mouse model, IL27RA<sup>-/-</sup>p53<sup>H/+</sup> (Fig. 5C,D) when compared to control treatment. The reduction of IL6 and TNF levels in the liver with ZD4054 inhibitor were also confirmed by ELISA (Fig. 5E,F).

Levels of mutant p53 protein, same as the WT one, are strictly regulated. The p53R172H protein in p53<sup>H/+</sup> mice is inherently unstable.<sup>(27,28)</sup> Because of the chronic unresolved inflammation in the liver IL27RA<sup>-/-</sup>p53<sup>H/+</sup>, one hypothesis is that the level of this p53-mutant protein is involved. In line with this hypothesis, both immunofluorescence (IF) and western blotting analysis revealed that p53 protein

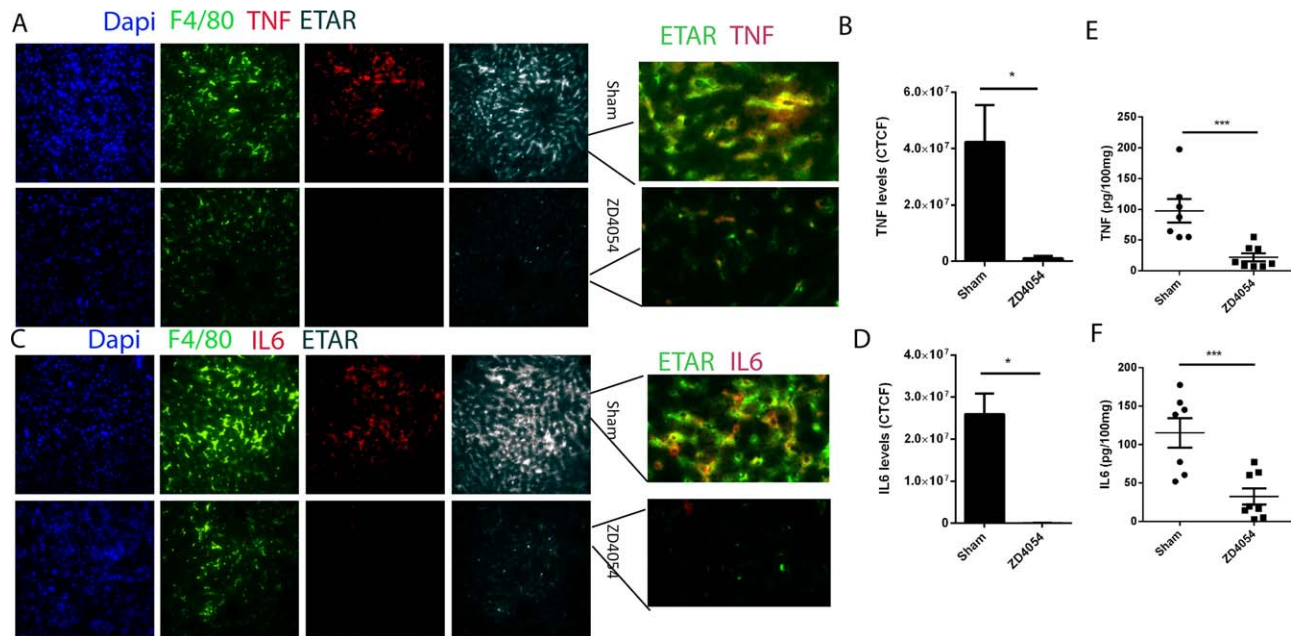


**FIG. 5.** ETAR signaling sustains inflammatory phenotype in the liver macrophages. (A) Triple staining for ETAR, F4/80, and TNF showed that inhibition of ETAR signaling reduced TNF levels in ETAR-positive macrophages. (B) Quantification of TNF staining. (C) Triple staining for ETAR, F4/80, and IL6 showed that inhibition of ETAR signaling reduced IL6 levels in ETAR-positive macrophages. (D) Quantification of IL6 staining. (E and F) Quantification of TNF and IL6 levels in liver by ELISA. Dots indicate data from liver of individual mice. Pictures taken at 200 $\times$ . \* $P < 0.05$ . Abbreviation: DAPI, 4',6'-diamidino-2-phenylindole.

accumulation were raised in IL27RA<sup>-/-</sup>p53<sup>H/+</sup> when compared to other control cohorts, though transcript levels remained the same (Fig. 6A-C). Meanwhile, p21 levels were low and similar between different cohorts, suggesting that WT p53 is unchanged in these cells (Supporting Fig. 5). These observations advocate the involvement of mutant p53 in chronic liver inflammation/fibrosis.

Because p53 stability is tightly linked to its function, and given the involvement of WT p53 in hepatocytes in the liver, next we sought to investigate in which cell type p53 is stabilized in liver of IL27RA<sup>-/-</sup>p53<sup>H/+</sup> mice. Surprisingly, mutant p53 is selectively stabilized in macrophages rather than in hepatocytes (Fig. 6D).

Whereas ETAR signaling in macrophages plays a substantial role in sustaining chronic and unresolved inflammation in liver of IL27RA<sup>-/-</sup>p53<sup>H/+</sup> mice, mechanistically how ETAR macrophages sustain chronic inflammation in the liver has not yet been investigated. Because p53 protein is accumulated mainly in macrophages, but not hepatocytes (Fig. 6D), we wanted to further investigate whether expression of mutant p53 in macrophages was a downstream target

from ETAR signaling. Indeed, ETAR induces pERK1/2 activation in our model (Fig. 4C,D), and others have shown that pERK1/2 can induce phosphorylation of p53 at Ser15, therefore enhancing its stability by preventing its interaction with MDM2.<sup>(29)</sup> Indeed, both IHC and western blotting confirmed that inhibition of ETAR results in diminished p53 accumulation, ERK1/2 phosphorylation, and phosphorylation of p53 at S15 (Fig. 6E,G, Fig. 7, and Supporting Fig. 6).

## Discussion

Unresolved chronic inflammation in the liver is tightly linked to fibrinogenesis; however, inflammatory pathways alone rarely cause chronic and unresolved inflammation. Indeed, these pathways aid the process of fibrinogenesis when induced by viruses or other inflammatory agents, but additional stimuli are needed to sustain unresolved inflammation. Involvement of oncogenic molecules, such as mutant p53, in this process remains elusive. More interesting, the combination of these two pathways has *never been examined* before this study. This novel investigation revealed that

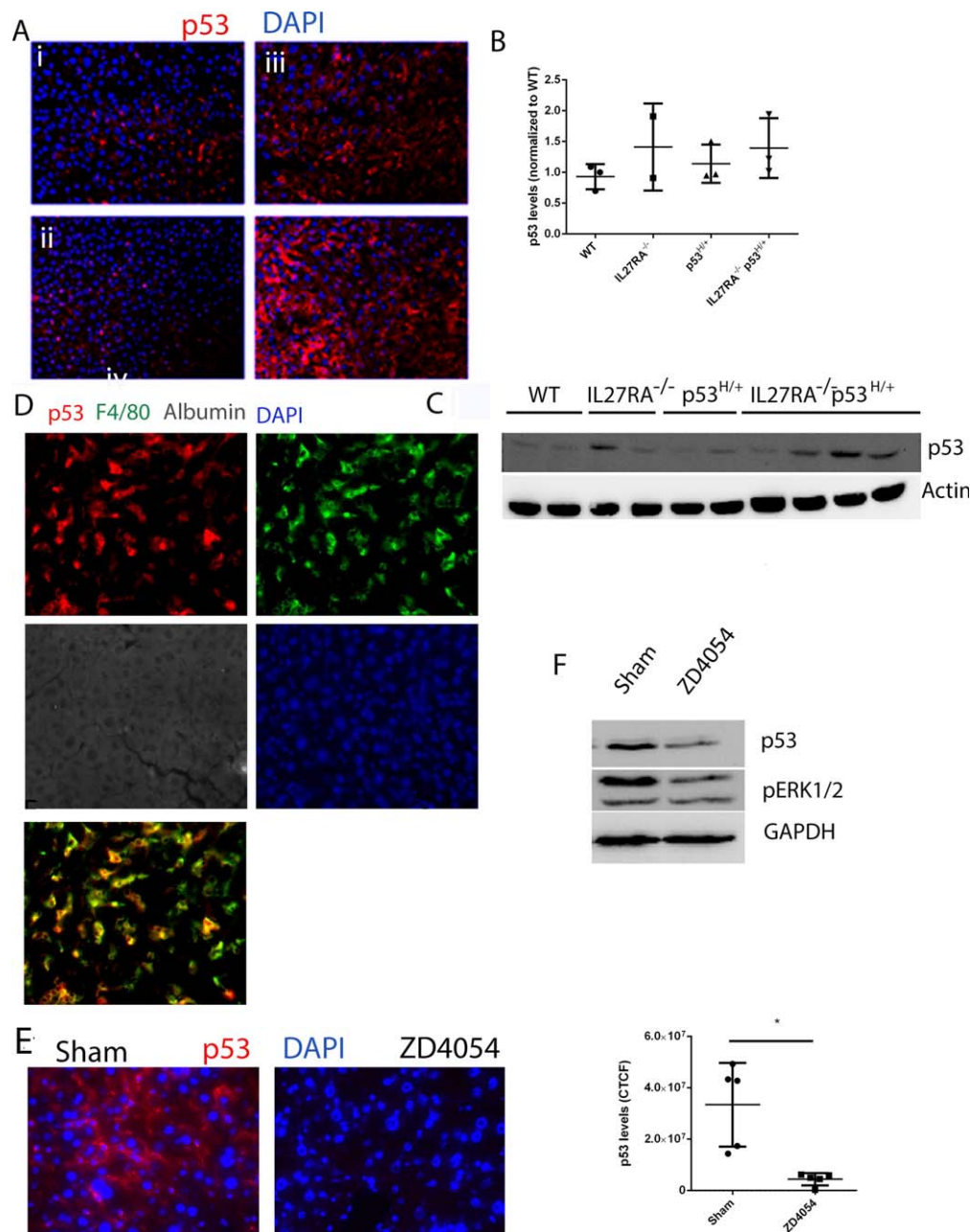


**FIG. 6.** p53 stability in macrophages is a downstream event of ETAR signaling. (A and B) IF and RT-PCR analysis showed that p53 protein accumulation, but not transcript levels, were raised in IL27RA<sup>-/-</sup>p53<sup>H/+</sup> when compared to other control cohorts in aged mice. (C) Western blotting showing increased p53 protein stability in aged livers of IL27RA<sup>-/-</sup>p53<sup>H/+</sup> when compared to age-matched genotypes. (D) Triple staining for p53, F4/80, and albumin showed that p53 is stabilized specifically in macrophages, but not hepatocytes. (E and F) Western blotting and IF staining showing that p53 levels (E) and pERK1/2 (F) levels are reduced in IL27RA<sup>-/-</sup>p53<sup>H/+</sup> mice treated with ZD4054 (N = 9), when compared to sham-treated mice (N = 7). *In vivo* data with ZD4054 inhibitor were repeated twice with similar results. Each lane or dot indicates data from liver of individual mice. Pictures taken at 200 $\times$ . \**P* < 0.05. Abbreviation: DAPI, 4',6-diamidino-2-phenylindole.

the combination of mutant p53<sup>R172H</sup> knock-in and an absence of IL27RA causes *spontaneous* chronic liver inflammation and steatosis in mice as they age whereas

expression of either genotype alone does not cause any liver inflammation or steatosis. Histologically, livers of these IL27RA<sup>-/-</sup>p53<sup>H/+</sup> mice closely reproduce

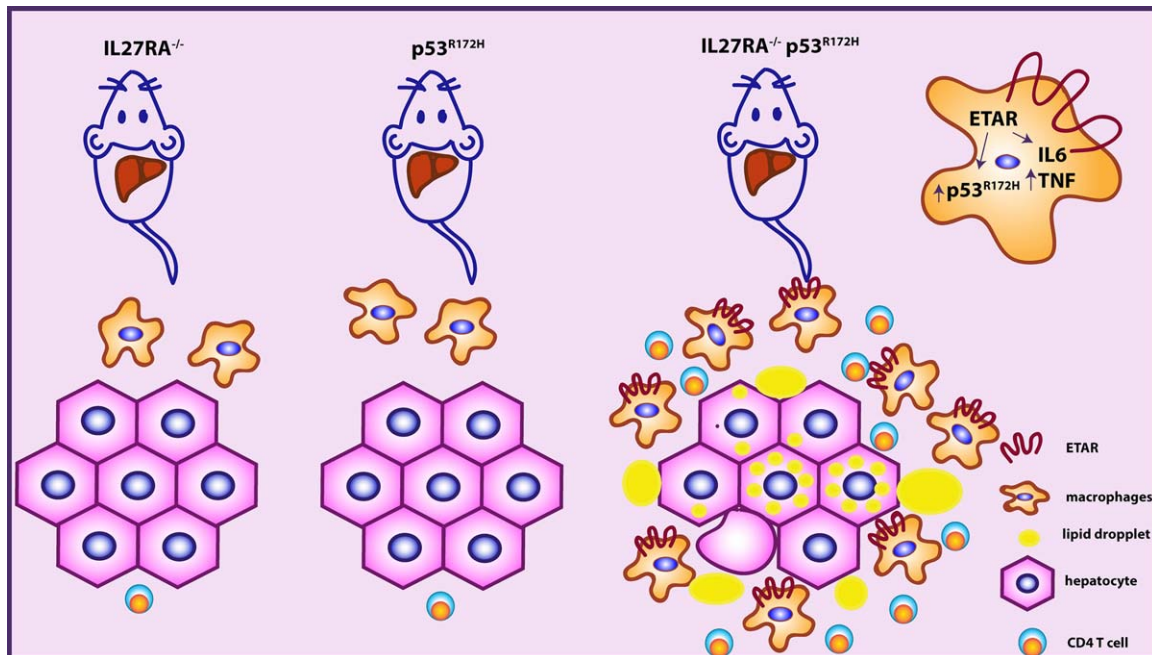


FIG. 7. Schematic overview of events that lead to liver disease in  $IL27RA^{-/-}p53^{H/+}$  mice.

features observed in nonalcoholic fatty liver disease (NAFLD)/NASH patients. Together, this information suggests a multiple-hit model for initiation and progression of unresolved chronic liver inflammation.

Two schools of thought exist on the driving forces of NAFLD/NASH. The first school suggests the sequential “two-hit” model, where steatosis is the first hit and inflammation is the second hit necessary to develop NASH.<sup>(30)</sup> Because only 10%–20% of patients that have NAFLD (benign disease) develop inflammation and fibrosis, Moschen et al. proposed that NASH might be a “separate disease with different pathogenesis.”<sup>(31)</sup> This group proposes that many hits might act in parallel, where inflammation may precede steatosis in NASH.<sup>(31)</sup> Some evidence for this hypothesis exists in that NASH patients present with little steatosis, and drugs targeting the inflammatory TNF pathway improve steatosis.<sup>(32,33)</sup> Meanwhile, genetic models that portray stepwise this multiple-hit hypothesis in the absence of hypernutrition have been limited. We believe that our genetic model supports the multiple-hit hypothesis: Inflammation occurs as early as 2–4 months, whereas accumulation of fat in the liver happens as a later event. Aside for histopathologically modeling NAFLD and NASH patients, this study further distinguished that ETAR-positive KCs

accumulate over time and play a significant role in this process. Furthermore, chemical inhibition of this ETAR pathway reverses inflammation and improves early signs of steatosis. (When the inhibitor studies were concluded at 5 months of age after 8 weeks of treatment, only early signs of steatosis were observed. The authors did not extend the inhibitor studies beyond 8 weeks because of the possibility of liver damage from extended use of the drug.) Another novel finding from this study was the phenotype developed in absence of hypernutrition. It is thought provoking that the genetic mouse model presented in this study might represent a different aspect of the NASH etiology that has not yet been appreciated, thereby adding to already established models and further contributing to the understanding of this disease in humans.

The overall understanding of ETAR-positive macrophages in liver pathogenesis is limited. The results reported here define ETAR-positive macrophages as the major contributor in sustaining liver inflammation in our model. Indeed, these cells were highly enriched in the liver of  $IL27RA^{-/-}p53^{H/+}$  mice, and inhibition of ETAR resolved or prevented accumulation of liver inflammatory foci (Fig. 4). Others have shown, by inhibition, that this pathway is indeed involved in liver pathogenesis. More concretely, inhibition of ETAR and

ETBR pathways in the liver significantly reverses liver fibrosis induced by CCL4. Similar to our finding that ET1 is increased in diseased livers in IL27RA<sup>-/-</sup>p53<sup>H/+</sup> mice, cirrhosis patients have much higher expression of ET1 when compared to healthy individuals, suggestive indeed of the clinical relevance of this pathway in liver pathogenesis.<sup>(25)</sup> Additionally, our study confirmed that the upstream molecular regulators, such as IL27RA<sup>-/-</sup> and mutant p53, are needed to sustain the accumulation of these proinflammatory macrophages in the liver (Fig. 4). Mechanistically, ETAR-positive macrophages sustaining inflammation in our model is closely associated with up-regulation of TNF and IL6 (Fig. 5), two well-characterized cytokines up-regulated in liver of NASH patients.<sup>(5,26)</sup>

An increase of p53 levels is closely associated with the ability of IL27RA<sup>-/-</sup>p53<sup>H/+</sup> mice to develop spontaneous inflammation (Fig. 6), which relates well with previously published results. In patient samples, p53 levels were significantly higher in those with steatohepatitis when compared to healthy individuals.<sup>(9)</sup> Most likely, mutant p53 is accumulating in our studies given that p21 levels were minimal among all different controls (Supporting Fig. 3). Other evidence exists in the literature coupling the activity of mutant p53 to inflammation. Under inflammatory conditions, intestinal stem cells expressing mutant p53 can proliferate at a faster rate than WT cells.<sup>(34)</sup> Furthermore, the p53R172H protein in p53<sup>H/+</sup> mice, similar to WT p53, is kept at basal levels. Multiple stress signals activate mutant p53 *in vivo*.<sup>(35)</sup> KCs are the predominant cell that displays p53 protein accumulation in liver of IL27RA<sup>-/-</sup>p53<sup>H/+</sup> mice (Fig. 6). ETAR signaling tightly regulated p53 levels in our model (Fig. 6). Most likely, ETAR-induced pERK1/2 will stabilize p53, given that others have shown that pERK1/2 activation enhances phosphorylation of p53 at serine 15, thereby reducing the affinity of this protein to interact with MDM2, the major ubiquitin ligase of p53.<sup>(29,36)</sup> Mutant p53 protein is involved in many steps from cancer initiation to progression, and in our model a similar phenomenon occurs, given that mutant p53 sustains KC numbers, which is, in turn, associated with hepatocyte necrosis and fibrosis, hallmarks of HCC development. HCC development did not occur in livers of these mice in our model, perhaps because of the shortened life span related to the rapid development of other tumors, such as sarcomas and lymphomas.

In this study, high p53 levels were observed in KCs of IL27RA<sup>-/-</sup>p53<sup>H/+</sup> mice when compared to other control genotypes; however, levels of p21 remained

basal in p53<sup>H/+</sup>, IL27RA<sup>-/-</sup>, and IL27RA<sup>-/-</sup>p53<sup>H/+</sup> mice, suggesting that mutant p53, rather than WT p53, is stabilized. This selective protein stabilization suggests the significance of mutant p53 protein in regulating the inflammation or ETAR expression in KCs in these mice. Such selective stabilization of mutant p53 is logical because an increased accumulation of WT p53 would cause apoptosis and elimination of these macrophages. Perhaps this mechanism exists in KCs of IL27RA<sup>-/-</sup> mice, which is why no increase expression of ETAR was found in liver of that mouse strain. Meanwhile, KCs from IL27RA<sup>-/-</sup>p53<sup>H/+</sup> mice stabilized mutant p53, and, most likely, these cells survive and accumulate over time because of a well-attributed, survival-dependent mechanism of mutant p53.

Our proof-of-principle study revealed that inflammatory macrophages with mitogenic or survival signals are contributors to chronic liver inflammation, steatosis, or steatohepatitis. This study linked mutant p53 to spontaneous and sustained liver inflammation and steatosis when combined with an inflammatory signal, such as the absence of IL27 signaling. Mechanistically, ETAR-positive macrophages are highly accumulated in the inflamed liver, and chemical inhibition of ETAR signaling reverses the observed phenotype and inflammatory cytokine levels, such as TNF and IL6. These results further contribute to our understanding of NAFLD/NASH in humans.

*Acknowledgment:* The authors are thankful to the pathologist, Dr. Laura Pigeon, and her histopathological readings.

## REFERENCES

- 1) Olive KP, Tuveson DA, Ruhe ZC, Yin B, Willis NA, Bronson RT, et al. Mutant p53 gain of function in two mouse models of Li-Fraumeni syndrome. *Cell* 2004;119:847-860.
- 2) Lang GA, Iwakuma T, Suh YA, Liu G, Rao VA, Parant JM, et al. Gain of function of a p53 hot spot mutation in a mouse model of Li-Fraumeni syndrome. *Cell* 2004;119:861-872.
- 3) Dibra D, Mishra L, Li S. Molecular mechanisms of oncogene-induced inflammation and inflammation-sustained oncogene activation in gastrointestinal tumors: an underappreciated symbiotic relationship. *Biochim Biophys Acta* 2014;1846:152-160.
- 4) Cooks T, Pateras IS, Tarcic O, Solomon H, Schetter AJ, Wilder S, et al. Mutant p53 prolongs NF-kappaB activation and promotes chronic inflammation and inflammation-associated colorectal cancer. *Cancer Cell* 2013;23:634-646.
- 5) Abiru S, Migita K, Maeda Y, Daikoku M, Ito M, Ohata K, et al. Serum cytokine and soluble cytokine receptor levels in patients with non-alcoholic steatohepatitis. *Liver Int* 2006;26:39-45.
- 6) Weisz L, Damalas A, Lontos M, Karakaidos P, Fontemaggi G, Maor-Aloni R, et al. Mutant p53 enhances nuclear factor

- kappaB activation by tumor necrosis factor alpha in cancer cells. *Cancer Res* 2007;67:2396-2401.
- 7) Scian MJ, Stagliano KE, Anderson MA, Hassan S, Bowman M, Miles MF, et al. Tumor-derived p53 mutants induce NF-kappaB2 gene expression. *Mol Cell Biol* 2005;25:10097-10110.
  - 8) Schneider G, Henrich A, Greiner G, Wolf V, Lovas A, Wiczorek M, et al. Cross talk between stimulated NF-kappaB and the tumor suppressor p53. *Oncogene* 2010;29:2795-2806.
  - 9) Akyol G, Dursun A, Poyraz A, Uluoglu O, Ataoglu O, Edaly N, Memis L. P53 and proliferating cell nuclear antigen (PCNA) expression in non-tumoral liver diseases. *Pathol Int* 1999;49:214-221.
  - 10) Panasiuk A, Dzieciol J, Panasiuk B, Prokopowicz D. Expression of p53, Bax and Bcl-2 proteins in hepatocytes in non-alcoholic fatty liver disease. *World J Gastroenterol* 2006;12:6198-6202.
  - 11) Attallah AM, Shiha GE, Ismail H, Mansy SE, El-Sherbiny R, El-Dosoky I. Expression of p53 protein in liver and sera of patients with liver fibrosis, liver cirrhosis or hepatocellular carcinoma associated with chronic HCV infection. *Clin Biochem* 2009;42:455-461.
  - 12) Loguerco C, Cuomo A, Tuccillo C, Gazzerro P, Cioffi M, Molinari AM, Del Vecchio Blanco C. Liver p53 expression in patients with HCV-related chronic hepatitis. *J Viral Hepat* 2003;10:266-270.
  - 13) Kodama T, Takehara T, Hikita H, Shimizu S, Shigekawa M, Tsunematsu H, et al. Increases in p53 expression induce CTGF synthesis by mouse and human hepatocytes and result in liver fibrosis in mice. *J Clin Invest* 2011;121:3343-3356.
  - 14) Lujambio A, Akkari L, Simon J, Grace D, Tschaharganeh DF, Bolden JE, et al. Non-cell-autonomous tumor suppression by p53. *Cell* 2013;153:449-460.
  - 15) Hunter CA, Kastelein R. Interleukin-27: balancing protective and pathological immunity. *Immunity* 2012;37:960-969.
  - 16) Chen Y, Jiang G, Yang HR, Gu X, Wang L, Hsieh CC, et al. Distinct response of liver myeloid dendritic cells to endotoxin is mediated by IL-27. *J Hepatol* 2009;51:510-519.
  - 17) Yamanaka A, Hamano S, Miyazaki Y, Ishii K, Takeda A, Mak TW, et al. Hyperproduction of proinflammatory cytokines by WSX-1-deficient NKT cells in concanavalin A-induced hepatitis. *J Immunol* 2004;172:3590-3596.
  - 18) Nagy ZS, LeBaron MJ, Ross JA, Mitra A, Rui H, Kirken RA. STAT5 regulation of BCL10 parallels constitutive NFkappaB activation in lymphoid tumor cells. *Mol Cancer* 2009;8:67.
  - 19) Dibra D, Cutrera J, Xia X, Kallakury B, Mishra L, Li S. Interleukin-30: a novel antiinflammatory cytokine candidate for prevention and treatment of inflammatory cytokine-induced liver injury. *HEPATOLOGY* 2012;55:1204-1214.
  - 20) Dibra D, Cutrera JJ, Xia X, Birkenbach MP, Li S. Expression of WSX1 in tumors sensitizes IL-27 signaling-independent natural killer cell surveillance. *Cancer Res* 2009;69:5505-5513.
  - 21) Mitra A, Satelli A, Yan J, Xueqing X, Gagea M, Hunter CA, et al. IL-30 (IL27p28) attenuates liver fibrosis through inducing NKG2D-rae1 interaction between NKT and activated hepatic stellate cells in mice. *HEPATOLOGY* 2014;60:2027-2039.
  - 22) Stienstra R, Saudale F, Duval C, Keshtkar S, Groener JE, van Rooijen N, et al. Kupffer cells promote hepatic steatosis via interleukin-1beta-dependent suppression of peroxisome proliferator-activated receptor alpha activity. *HEPATOLOGY* 2010;51:511-522.
  - 23) Wolf MJ, Adili A, Piotrowitz K, Abdullah Z, Boege Y, Stemmer K, et al. Metabolic activation of intrahepatic CD8+ T cells and NKT cells causes nonalcoholic steatohepatitis and liver cancer via cross-talk with hepatocytes. *Cancer Cell* 2014;26:549-564.
  - 24) Gandhi CR, Nemoto EM, Watkins SC, Subbotin VM. An endothelin receptor antagonist TAK-044 ameliorates carbon tetrachloride-induced acute liver injury and portal hypertension in rats. *Liver* 1998;18:39-48.
  - 25) Pinzani M, Milani S, DeFranco R, Grappone C, Caligiuri A, Gentilini A, et al. Endothelin 1 is overexpressed in human cirrhotic liver and exerts multiple effects on activated hepatic stellate cells. *Gastroenterology* 1996;110:534-548.
  - 26) Bahcecioglu IH, Yalniz M, Ataseven H, Ilhan N, Ozercan IH, Seckin D, Sahin K. Levels of serum hyaluronic acid, TNF-alpha and IL-8 in patients with nonalcoholic steatohepatitis. *Hepato-gastroenterology* 2005;52:1549-1553.
  - 27) Suh YA, Post SM, Elizondo-Fraire AC, Maccio DR, Jackson JG, El-Naggar AK, et al. Multiple stress signals activate mutant p53 in vivo. *Cancer Res* 2011;71:7168-7175.
  - 28) Terzian T, Suh YA, Iwakuma T, Post SM, Neumann M, Lang GA, et al. The inherent instability of mutant p53 is alleviated by Mdm2 or p16INK4a loss. *Genes Dev* 2008;22:1337-1344.
  - 29) Melnikova VO, Santamaria AB, Bolshakov SV, Ananthaswamy HN. Mutant p53 is constitutively phosphorylated at Serine 15 in UV-induced mouse skin tumors: involvement of ERK1/2 MAP kinase. *Oncogene* 2003;22:5958-5966.
  - 30) Day CP, James OF. Steatohepatitis: a tale of two "hits"? *Gastroenterology* 1998;114:842-845.
  - 31) Tilg H, Moschen AR. Evolution of inflammation in nonalcoholic fatty liver disease: the multiple parallel hits hypothesis. *HEPATOLOGY* 2010;52:1836-1846.
  - 32) Tiniakos DG, Vos MB, Brunt EM. Nonalcoholic fatty liver disease: pathology and pathogenesis. *Annu Rev Pathol* 2010;5:145-171.
  - 33) Li Z, Yang S, Lin H, Huang J, Watkins PA, Moser AB, et al. Probiotics and antibodies to TNF inhibit inflammatory activity and improve nonalcoholic fatty liver disease. *HEPATOLOGY* 2003;37:343-350.
  - 34) Vermeulen L, Morrissey E, van der Heijden M, Nicholson AM, Sottoriva A, Buczacki S, et al. Defining stem cell dynamics in models of intestinal tumor initiation. *Science* 2013;342:995-998.
  - 35) Suh YA, Post SM, Elizondo-Fraire AC, Maccio DR, Jackson JG, El-Naggar AK, et al. Multiple stress signals activate mutant p53 in vivo. *Cancer Res* 2011;71:7168-7175.
  - 36) Haupt Y, Maya R, Kazaz A, Oren M. Mdm2 promotes the rapid degradation of p53. *Nature* 1997;387:296-299.

## Supporting Information

Additional Supporting Information may be found at [onlinelibrary.wiley.com/doi/10.1002/hep.28379/supinfo](http://onlinelibrary.wiley.com/doi/10.1002/hep.28379/supinfo).